

Semi-DerainGAN: A New Semi-supervised Single Image Deraining Network

Yanyan Wei¹, Zhao Zhang¹, Haijun Zhang², Jie Qin³ and Mingbo Zhao⁴

¹Hefei University of Technology, ²Harbin Institute of Technology (Shenzhen), ³ETH Zürich,

⁴City University of Hong Kong, E-mail: cszzhang@gmail.com

Abstract

Removing the rain streaks from single image is still a challenging task, since the shapes and directions of rain streaks in the synthetic datasets are very different from real images. Although supervised deep deraining networks have obtained impressive results on synthetic datasets, they still cannot obtain satisfactory results on real images due to weak generalization of rain removal capacity, i.e., the pre-trained models usually cannot handle new shapes and directions that may lead to over-derained/under-derained results. In this paper, we propose a new semi-supervised GAN-based deraining network termed Semi-DerainGAN, which can use both synthetic and real rainy images in a uniform network using two supervised and unsupervised processes. Specifically, a semi-supervised rain streak learner termed *SSRML* sharing the same parameters of both processes is derived, which makes the real images contribute more rain streak information. To deliver better deraining results, we design a paired discriminator for distinguishing the real pairs from fake pairs. Note that we also contribute a new real-world rainy image dataset Real200 to alleviate the difference between the synthetic and real image domains. Extensive results on public datasets show that our model can obtain competitive performance, especially on real images.

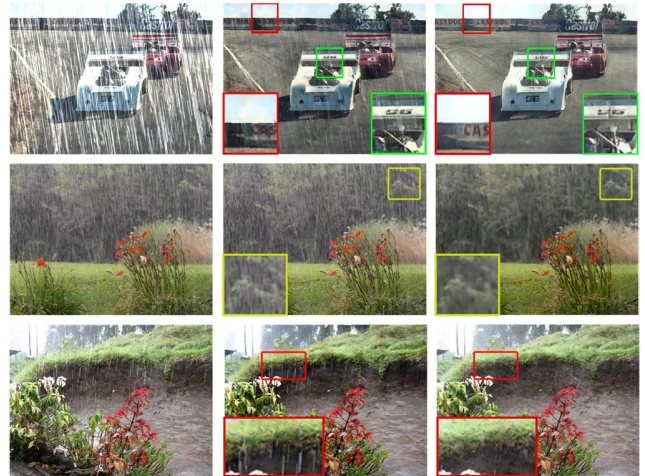
1 Introduction

Single image deraining (SID) is a challenging and interesting topic in the areas of computer vision and artificial intelligence due to its broad realistic application areas, e.g., drone-based video surveillance, real-time object recognition and autonomous cars. The problem of SID can be modeled as follows:

$$X = R + B, \quad (1)$$

where X denotes a rainy image to be decomposed into a rain-streak component R and a clean background B , i.e., removing the rain streaks from rainy images. Since Eqn. (1) is an ill-posed problem, some feasible methods have been proposed to solve it, include both traditional and deep learning-based models, which will be introduced briefly in Section 2.

It is noteworthy that most existing deep deraining networks are supervised using paired information in synthetic datasets. The strong constraint can make the network convergence fast



(a) original images (b) result of SSSL (c) our result

Figure 1. Comparison of the deraining results of Semi-DerainGAN and SSSL [Wei *et al.*, 2019] on both the synthetic images (first row) and real rainy images (second row). We see that our network performs better on both datasets, while SSSL leaves more rain streaks.

on synthetic images, however, the performance on the real-world rainy images is still unsatisfactory. To address this problem, some researchers start to shift to study the semi-supervised deraining models, which can also use real images to enhance the generalization ability. For example, a semi-supervised SID framework called Semi-Supervised Transfer Learning (SSTL) [Wei *et al.*, 2019] was recently proposed to solve the problem mentioned above. Different from traditional methods that only use the supervised image pairs with artificial synthetic rain, SSTL further adds the real rainy images without clean images (ground-truth) for the network training. This is achieved by taking the residual between the input rainy image and expected network output (clear image without rain) as a specific parameterized rain fringe distribution. As such, SSTL adapts to the real unsupervised rain types by transferring the supervised synthetic rain, which can clearly alleviate the issue of insufficient training data and supervised sample bias. But the rain streaks in synthetic and real images are very different, so it may be unsuitable to train synthetic and real-world images by adding a constraint between synthetic rain and real rainy image domains in a single network, i.e., minimizing the KL divergence between a synthetic

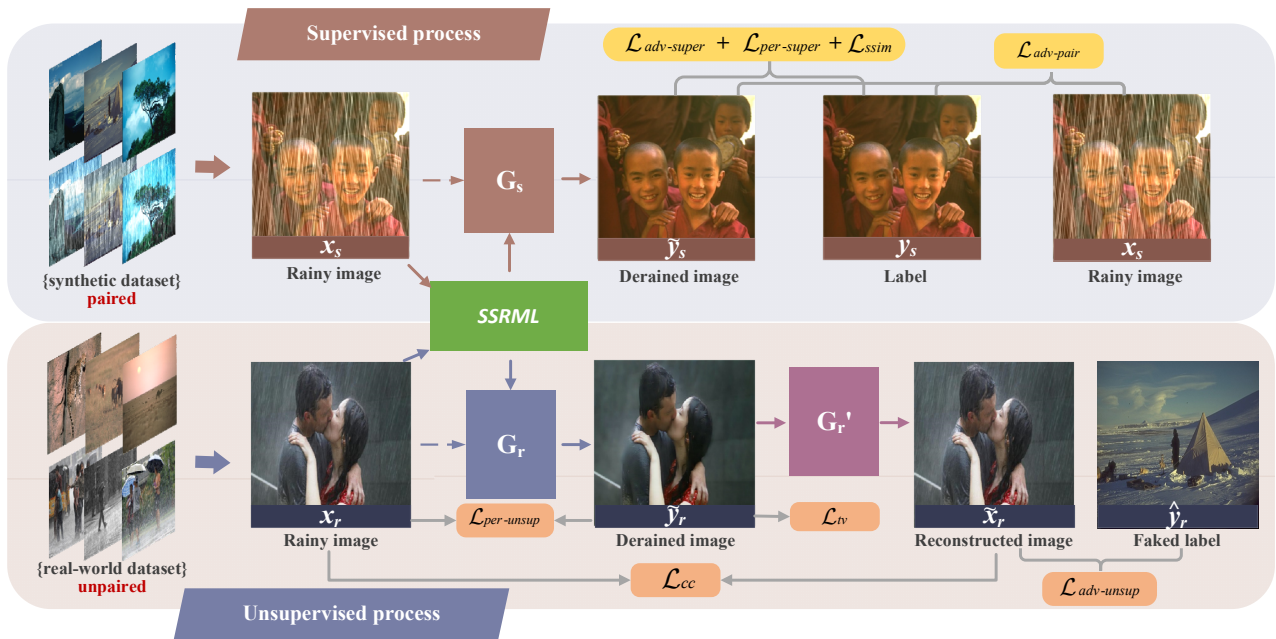


Figure 2. The framework of our Semi-DerainGAN that includes two processes, i.e., supervised and unsupervised processes. The supervised process is for synthetic image training by minimizing the losses of \mathcal{L}_{super} denoted in gold color, while the unsupervised process is for real-world image training by minimizing the losses of \mathcal{L}_{unsup} denoted in orange color. The semi-supervised rain mask learner $SSRML$ is a shared module that can learn the rain streak information from both the synthetic and real-world rainy images.

rain streak mask and real one learned from real images in training. Note that KL divergence is the most important part of SSTL, which can prompt the semi-supervised model work. So SSTL may leave rain streaks in deraining process on both synthetic and real-world data (see Fig.1).

In this paper, we therefore propose a new semi-supervised SID network that use two processes to train synthetic and real images respectively by a hybrid loss, which can solve the issues mentioned above. The contributions are summarized as:

(1) A new semi-supervised single image deraining method, termed Semi-DerainGAN, is technically proposed. Semi-DerainGAN can use both synthetic rainy images and real rainy images in a uniform network by two divided processes (i.e., supervised and unsupervised processes). In this manner of two divided process, Semi-DerainGAN can avoid degraded interaction in a single network (e.g., SSTL), which is caused by rain streak information of two different domains (i.e., synthetic and real-world domains). To the best of our knowledge, this is one of few semi-supervised deep models for SID, and also this is the first work using GAN for semi-supervised SID.

(2) Semi-DerainGAN has two processes, i.e., supervised and unsupervised ones. The supervised process is for the synthetic image training, while the unsupervised process is for real image training. Specifically, a semi-supervised rain mask learner ($SSRML$) is used to learn rain streak information from both synthetic and real rainy images, and two generators for two independent generation processes are used to generate the derained images by training. The two processes can alleviate the degradation issue caused by the difference between rain streaks in synthetic and real image domains.

(3) A new real rainy image dataset Real200 is also created to alleviate the difference between the two domains. To the best of our knowledge, this is the first real rainy image dataset with carefully-selected rain streak directions and shapes. Due to the attractive properties of Real200, we see experimentally that it can improve the semi-supervised SID clearly.

(4) Extensive experiments on several challenging synthetic datasets and real images demonstrate the effectiveness of our Semi-DerainGAN for semi-supervised SID, compared with that of semi-supervised method SSTL.

2 Related Work

To solve the SID problem, many traditional algorithms have been proposed, e.g., low-rank representation methods (e.g., [Zhang and Patel, 2017]), Gaussian mixture models (GMM) (e.g., [Li *et al.*, 2016]), and sparse coding-based models (e.g., [Luo *et al.*, 2015]). In recent years, some deep learning-based deep network models were proposed. For example, a contextualized dilated network [Yang *et al.*, 2017] was recently proposed to jointly detect and remove the rain streaks from single image. [Fu *et al.*, 2017] uses the residual block [He *et al.*, 2016] to reduce the mapping range from input to output directly, which makes the learning process easier. A novel density-aware multi-stream dense convolutional network-based framework [Zhang and Patel, 2018] was proposed to jointly estimate the rain density and deraining. More recently, a hybrid block [Wei *et al.*, 2019] was proposed to extract the rain streak more precisely, especially in heavy rainy condition.



Figure 3. Real images in two datasets (SSTL-Data and Real200). In (a), the first row is the original real rainy image from Internet and the second row shows cropped ones suitable for semi-supervised learning. In (b), from the top left to bottom right are snow weather, low resolution, mist weather and bright region respectively.

Due to the powerful capacity of generating realistic images, Generative Adversarial Networks (GAN) [Goodfellow *et al.*, 2014] have achieved superior performance in many vision tasks, including the SID. [Zhang *et al.*, 2017] proposed a conditional GAN-based network model which considers quantitative, visual and discriminative performance into the objective function. [Qian *et al.*, 2018] proposed a raindrop removal method which uses GAN to produce the attention map by an attentive-recurrent network and uses it to generate a raindrop-free image through a contextual auto-encoder. Note that these existing GAN-based models are supervised ones which need paired data for training, so they are hard to be used in semi-supervised and unsupervised modes. To solve the restrictions on the conditions of using GAN, CycleGAN [Zhu *et al.*, 2017] was proposed by using unpaired data in training process, which can translate an image from a source domain X to a target domain Y and then reconstruct it from the domain Y to domain X , formulated as $X \rightarrow Y \rightarrow X$. In our network, we use the CycleGAN for our unsupervised process.

3 Proposed Semi-DerainGAN

3.1 Network Architecture

We illustrate the framework of our Semi-DerainGAN in Fig.2 which has two supervised and unsupervised processes. The framework has a semi-supervised rain mask learner (*SSRML*), three generators (G_s, G_r, G_r') that dispose on the synthetic rain images and real rainy images respectively and three discriminators (D_s, D_r, D_p) corresponding to the generators. The synthetic and real rainy images are denoted as $\{x_s^i, y_s^i\}_{i=1}^{M_s} \in S$ and $\{x_r^i, y_r^i\}_{i=1}^{N_r} \in R$, respectively, where x_s and y_s are rainy image and its corresponding rain-free image (i.e., label) in synthetic dataset S , while x_r and y_r are rainy image and corresponding rain-free image in real dataset R . Since x_r has no corresponding ground truth, we randomly choose \hat{y}_r from $\{y_s^i\}_{i=1}^{M_s} \in S$ as the ground truth (i.e., fake label). In what follows, we will introduce detailed information of each part respectively.

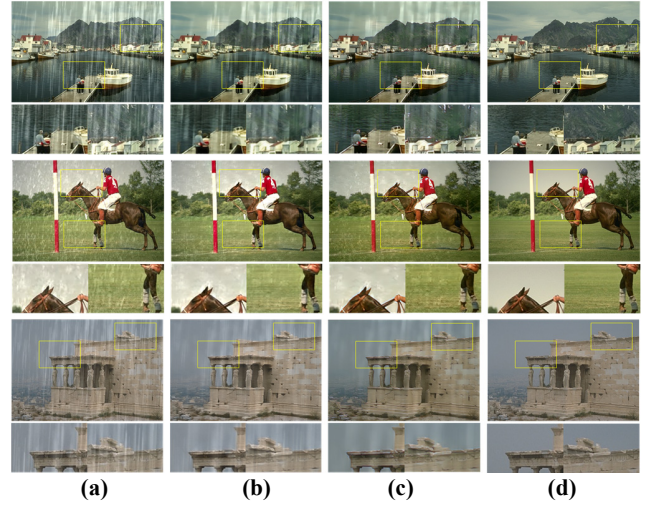


Figure 4. Comparison of deraining results on Rain1400 [Fu *et al.*, 2017] and SSTL-Data [Wei *et al.*, 2019], where (a) input rain image, (b) result of SSTL, (c) result of our method, and (d) ground-truth.

(1) Semi-supervised Rain Mask Learner (*SSRML*)

The original rain mask learner (*RML*), as an attentional rain drops extractor by [Qian *et al.*, 2018], performs in supervised mode, which includes a *LSTM* unit and five *Conv-Relu-Conv-Relu* units. Due to the supervised nature of *RML*, it needs all paired data that are not easy to be obtained in reality, which will directly restrict its real applications. To address this issue, we design a structure to use *RML* as an attentional rain streak extractor in semi-supervised mode, called semi-supervised rain mask learner (*SSRML*), to learn rain streak information (i.e., shapes and directions) from both the synthetic and real-world rain image domains. Under the circumstances, *SSRML* can obtain better deraining result in the real-world SID task. Overall, this process can be formulated as

$$m_s = SSRML(x_s), m_r = SSRML(x_r), \quad (2)$$

where m_s and m_r are the rain masks extracted from synthetic rainy image x_s and real rainy image x_r , respectively.

(2) Generators in Synthetic and Real Image Domains

We describe the three generators G_s, G_r, G_r' in our network. Specifically, G_s and G_r can generate the derained images from synthetic data S and real-world data R in training process respectively, and we utilize the U-net [Qian *et al.*, 2018]. Then, G_r' reconstructs the real rainy image for a consist purpose which is proposed in CycleGAN [Zhu *et al.*, 2017], and is consisted of a *SSRML* and a U-net. The formulation for the generators can be represented as follows:

$$\tilde{y}_s = G_s(m_s, x_s), \tilde{y}_r = G_r(m_r, x_r), \tilde{x}_r = G_r'(\tilde{y}_r), \quad (3)$$

where \tilde{y}_s and \tilde{y}_r are the derained results of images x_s and x_r , and \tilde{x}_r is reconstructed rainy image of the derained image \tilde{y}_r .

(3) Discriminators in Synthetic and Real Image Domains

We introduce the three discriminators D_s, D_r, D_p in our model, which have two types of discriminators. The first type contains D_s and D_r that apply multi-scale structures, where the

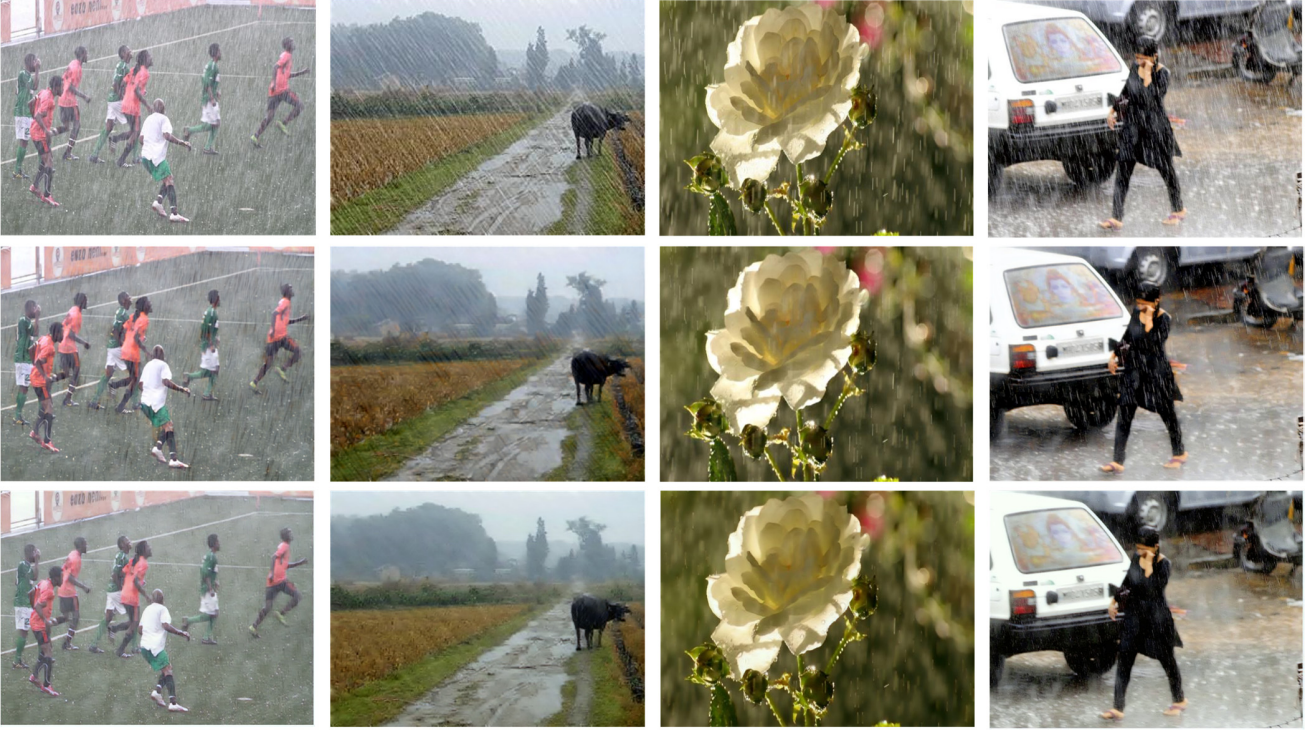


Figure 5. Comparison of the semi-supervised SID results on real-world images. The first row denotes the original real-world rainy images, the second and third rows denote the deraining results of SSTL and our network, respectively.

feature maps at each scale go through five convolution layers and then are fed into sigmoid outputs [Lee *et al.*, 2018]. We use 3 different scales for D_s and D_r . The second type of discriminator D_p is a paired discriminator [Gu *et al.*, 2019] proposed for the makeup transforming. In our network, we simplify the input of D_p and use paired images, i.e., rainy and derained images, to make the network generate more realistic derained images. The efficiency of the paired discriminator is verified by simulations. The adversarial losses for used generators and discriminators can be defined as follows:

$$\begin{aligned} \mathcal{L}_{adv-super} = & \mathbb{E}_{x_s \sim S} [\log D_s(y_s)] \\ & + \mathbb{E}_{x_s \sim S} [\log (1 - D_s(G_s(SSRML(x_s), x_s)))] \\ & + \mathcal{L}_{adv-pair} \end{aligned} \quad (4)$$

$$\begin{aligned} \mathcal{L}_{adv-pair} = & \mathbb{E}_{x_s \sim S} [\log D_p(x_s, y_s)] \\ & + \mathbb{E}_{x_s \sim S} [\log (1 - D_p(x_s, (G_s(SSRML(x_s), x_s))))] \\ \mathcal{L}_{adv-unsup} = & \mathbb{E}_{x_r \sim R} [\log D_r(\hat{y}_r)] + \\ & + \mathbb{E}_{x_r \sim R} [\log (1 - D_r(G_r(SSRML(x_r), x_r)))] \end{aligned} \quad (5)$$

where $\mathcal{L}_{adv-super}$ is the adversarial loss which contains a loss of pair discriminator $\mathcal{L}_{adv-pair}$ for the supervised learning process and $\mathcal{L}_{adv-unsup}$ is an adversarial loss for unsupervised process.

3.2 Supervised Process

The proposed Semi-DerainGAN will be trained using both the supervised and unsupervised processes synchronously. In the supervised process, we use synthetic data $\{x_s^i, y_s^i\}_{i=1}^{M_s} \in S$ to learn the parameters of network, i.e., $SSRML, G_s, D_s$ and D_p . We minimize the following supervised loss function:

$$\mathcal{L}_{super} = \lambda_{adv-super} \mathcal{L}_{adv-super} + \lambda_{per-super} \mathcal{L}_{per-super} + \lambda_{ssim} \mathcal{L}_{ssim}, \quad (6)$$

where $\mathcal{L}_{adv-super}$ is an adversarial loss for this process in Eqn. (4), $\mathcal{L}_{per-super}$ denotes the perceptual loss [Johnson *et al.*, 2016] that can encode the difference between derained image \tilde{y}_s and the corresponding label image y_s , \mathcal{L}_{ssim} is the *SSIM* loss [Wang *et al.*, 2004] that can keep structural similarity between the two images, $\lambda_{adv-super}$, $\lambda_{per-super}$ and λ_{ssim} are tradeoff parameters to control the contributions of each loss. Note that the two losses $\mathcal{L}_{per-super}$ and \mathcal{L}_{ssim} can be defined as follows:

$$\mathcal{L}_{per-super} = \|\partial_v(y_s) - \partial_v(\tilde{y}_s)\|_2^2, \quad (7)$$

$$\mathcal{L}_{ssim} = -SSIM(y_s, \tilde{y}_s), \quad (8)$$

where $\partial_v(\cdot)$ denotes the feature extractor of the *conv2.3* layer of VGG-16 network [Simonyan and Zisserman, 2015] that are pre-trained on ImageNet [Deng *et al.*, 2009]. *SSIM*(\cdot) is the *SSIM* function to calculate the similarity between two images y_s and \tilde{y}_s . Note that we aim at maximizing the *SSIM* value as much as possible, so \mathcal{L}_{ssim} is a negative function.

Dataset	Input	Rain1400					Rain1400&SSTL-Data		
		DSC	GMM	DDN	JORDER	DID-MDN	SSTL	Our w/o R	Our
Sparse	24.14	25.05	25.67	26.88	24.22	25.66	26.98	26.15	27.48
Dense	17.95	19.00	19.27	19.90	18.75	18.60	21.60	20.32	22.25

Table 1. Comparison with each model in terms of PSNR on Rain1400 and Rain1400&SSTL-Data. **Bold** denotes the best performance. *w/o R* means that only using the synthetic dataset Rain1400, i.e., trained in supervised mode.

3.3 Unsupervised Process

In the unsupervised process, we use the real-world rain image data $\{x_r^i, \hat{y}_r^i\}_{i=1}^{N_r} \in R$ to learn the parameters of the network, i.e., $SSRML, G_r, \hat{G}_r$ and D_r . Specifically, we minimize the following unsupervised loss function:

$$\mathcal{L}_{unsup} = \lambda_{adv-unsup} \mathcal{L}_{adv-unsup} + \lambda_{cc} \mathcal{L}_{cc} + \lambda_{per-unsup} \mathcal{L}_{per-unsup} + \lambda_{tv} \mathcal{L}_{tv}, \quad (9)$$

where $\mathcal{L}_{adv-unsup}$ is the adversarial loss for unsupervised process, \mathcal{L}_{cc} ensures that the derained image \hat{y}_r can be translated back to the original rainy image x_r for preserving the contents of images [Zhu *et al.*, 2017], $\mathcal{L}_{per-unsup}$ similarly defined as $\mathcal{L}_{per-sup}$, $TV(\cdot)$ is the TV function to make generated real derained image more realistic. $\lambda_{adv-unsup}, \lambda_{cc}, \lambda_{per-unsup}$ and λ_{tv} are the trade-off parameters to balance the losses. Technically, $\mathcal{L}_{cc}, \mathcal{L}_{per-unsup}$ and \mathcal{L}_{tv} can be defined as follows:

$$\mathcal{L}_{cc} = \mathbb{E}_{x_r \sim R} [\|x_r - \tilde{x}_r\|_1], \quad (10)$$

$$\mathcal{L}_{per-unsup} = \|\partial_v(x_r) - \partial_v(\hat{y}_r)\|_2^2, \quad (11)$$

$$\mathcal{L}_{tv} = TV(\hat{y}_r). \quad (12)$$

3.4 Objective Function

The overall loss function of Semi-DerainGAN used for training the proposed network is defined as follows:

$$\mathcal{L}_{total} = \mathcal{L}_{super} + \lambda_{unsup} \mathcal{L}_{unsup}, \quad (13)$$

where λ_{unsup} is a tradeoff parameter to balance the supervised process \mathcal{L}_{super} and unsupervised process \mathcal{L}_{unsup} .

3.5 Created Real Rainy Image Dataset Real200

For SID, most existing rainy image datasets are synthetic, [Wei *et al.*, 2019] have proposed a real-world dataset that is called SSTL-Data in this paper, which has 147 real rainy images. However, SSTL-Data has three drawbacks: (1) it has many unsuitable weather conditions, including snow weather, mist weather, which can hardly prompt the convergence in semi-supervised SID training process and even has the negative effect; (2) it contains some low-resolution images whose rain streaks can hardly be recognized; (3) these images are raw and un-treated, which may contain rain-free regions, or too light to see the rain streaks in sky or rainwater ground, or containing rain drops or rain spray. Maybe researchers think that these situations can enhance the generalization ability of network, but in fact it may be meaningless and even negative for training. Although these images are realistic, they are unsuitable for the semi-supervised mode. In other words, if we could solve the drawbacks of SSTL-Data, we can train a better semi-supervised model in same setting. As such, we create

Datasets	Rain100H		Rain100L		Rain12	
Metrics	PSNR	SSIM	PSNR	SSIM	PSNR	SSIM
DSC	13.77	0.320	27.34	0.849	30.07	0.866
GMM	15.23	0.450	29.05	0.872	32.14	0.916
DDN	22.85	0.725	32.38	0.926	34.04	0.933
SSTL*	22.47	0.716	32.37	0.925	34.02	0.935
Ours*	22.89	0.801	34.12	0.958	35.86	0.960

Table 2. Quantitative comparison on three synthetic datasets. Since SSTL is a semi-supervised network, the comparison with it will be most meaningful. * denotes that the model trained on specified synthetic dataset plus SSTL-Data. **Bold** denotes the best performance.

a new real-world rainy image dataset called Real200, which is elaborately selected from real-world rainy images and is manually cropped to highlight the rainy regions (see Fig.3).

The advantages of Real200 are that it only has rainy condition and each image has high resolution, it is cropped manually to highlight rain streak regions while preserving the diversity of the rain streaks in real-world images. Note that the rain streaks of Real200 are not significantly different from those in synthetic rainy images, so it will be beneficial to the training of a semi-supervised model, as can be seen in Table 4. Due to the positive effect of this real dataset, it can be used in the subsequent semi-supervision SID tasks.

4 Experimental Results and Analysis

4.1 Training Details

The proposed network is trained using Pytorch [Paszke *et al.*, 2017] in Python environment on a NVIDIA GeForce GTX 1080i GPU with 12GB memory. We crop each rainy image to many patches of 100×100 by stride of 80. Adam [Kingma and Ba, 2015] is used as the optimization algorithm with a batch size of 4. The model is trained for total 200 epochs. The learning rate of supervised process and unsupervised process is set to 1e-4 and 1e-3, respectively. The learning rate is decayed with a policy of Pytorch after 100 epochs. The trade-off parameters in Eqns. (6) and (13) are set to 1, and the trade-off parameters in Eqn. (9) are set to 1.5e-5, 10, 1 and 100, respectively. All tradeoff parameters are chosen empirically.

4.2 Datasets and Evaluation Metrics

Synthetic and Real-world Rainy image Datasets

Four synthetic datasets are used in this study: (1) Rain100H [Yang *et al.*, 2017] that has five streak directions, contains 1,800 rainy images for training and 100 rainy images for testing; (2) Rain100L [Yang *et al.*, 2017], where 200 image pairs are used for training and 100 image pairs are for testing; (3) Rain1400 [Fu *et al.*, 2017] has 14000 pairs of rainy images with 14 kinds of different rain streak orientations and magnitudes; (4) Rain12 [Li *et al.*, 2016] contains 12 rainy and clean

Setting	w/o. \mathcal{L}_{per}	w/o. \mathcal{L}_{iv}	w/o. D_p	$\mathcal{L}_{total} + D_p$
PSNR	32.25	33.82	29.94	34.12
SSIM	0.939	0.964	0.949	0.958

Table 3. Deraining results of our method with different settings on Rain100L&SSTL-Data, where w/o means without specified loss or module. **Bold** denotes the best performance.

image pairs. Since Rain12 has few samples, we directly apply the trained network model on Rain100L to test it.

For real-world images, we use two datasets in our paper: (1) SSTL-Data [Wei et al., 2019] which contains 147 real-world rainy images; (2) Real200 that is created in this paper, which contains 200 real-world rainy images. Since our method and SSTL are semi-supervised methods, we use synthetic dataset plus real-world dataset for training, which is denoted by &, such as Rain1400&SSTL-Data and Rain100L&Real200.

Evaluation Metrics and Compared Methods

Peak Signal-to-Noise Ratio (PSNR) [Huynh-Thu and Ghanbari, 2008] and the Structural Similarity Index (SSIM) [Wang et al., 2004] are used for evaluating the images with ground-truth. For real-world images that have no ground-truth, such as SSTL-Data, we only provide the visual deraining results.

Six SID models are compared with, including two model-driven methods (i.e., DSC [Luo et al., 2015] and GMM [Li et al., 2016]), three supervised deep learning models (i.e., DDN [Fu et al., 2017], JORDER [Yang et al., 2017] and DID-MDN [Zhang and Patel, 2018]), and one semi-supervised deep learning model (i.e., SSTL [Wei et al., 2019]).

4.3 Results on Synthetic Rainy images

We first evaluate each method on the Rain1400&SSTL-Data, which contains a total 14000 pairs of synthetic rain images plus 147 real-world rain images for training and we use other 20 images (10 sparse rain streak and 10 dense rain streak images) for testing. The supervised models are directly trained on Rain1400, and the semi-supervised models are trained on Rain1400&SSTL-Data. For the fair comparison, we directly use the deraining results from SSTL [Wei et al., 2019]. From Table 1, one sees that our network can achieve the best performance on both sparse and dense test data. To show the effect of unsupervised process in our model, we also train our model in a supervised mode totally (i.e., without real-world data). The result shows that the performance of adding real-world images for training in two process can be improved. The illustration of deraining results also can be seen in Fig. 4. We also perform each model on other synthetic datasets in Table 2 and directly adopts the results of [Wang et al., 2019]. The results also demonstrate superior performance of our network over other compared methods.

4.4 Results on Real Rainy images

We mainly compare the semi-supervised deraining results of our network with those of SSTL on Rain1400&SSTL-Data. Note that we aim at visualizing the derained results in Fig.5, from which we can see that our network performs better than SSTL obviously, since SSTL leaves more rain streaks, which keeps consistent with the above numerical results.

Datasets	Rain100L&SSTL-Data		Rain100L&Real200	
Metrics	PSNR	SSIM	PSNR	SSIM
Our model	34.12	0.958	35.27	0.970

Table 4. Comparison of the deraining result of Semi-DerainGAN on Rain100L&SSTL-Data and Rain100L&Real200, respectively. It is clear that the results on Rain100L&Real200 are better than that on Rain100L&SSTL-Data. That is, our contributed real rain image dataset Real200 can enhance the semi-supervised deraining. **Bold** denotes the best performance.

4.5 Ablation Study

We discuss the loss functions and module in our network, and demonstrate the availability of our created real rain image dataset Real200. To reduce the time consumption for training, we simply use Rain100L& SSTL-Data as the training data.

Loss Functions and Module

We first explore the deraining results of our network without $\mathcal{L}_{per} = \mathcal{L}_{per-unsup} + \mathcal{L}_{per-super}$ or \mathcal{L}_{iv} in Table 3, from which we see that the performance goes down without partial loss, especially on the metric of PSNR. Besides, we evaluate the importance of D_p in our network, and we can see that without D_p , the resulted performance drops fast.

Evaluation on SSTL-Data and Our Real200

We investigate the effectiveness of the created real rainy image dataset Real200 for semi-supervised SID. As can be seen in Table 4, the deraining results of our Semi-DerainGAN on Rain100L&Real200, which is a mixed dataset with Rain100L and Real200, is clearly better than it on Rain100L&SSTL-Data that is a mixed dataset with Rain100L and SSTL-Data. That is, our created new Real200 dataset can provide more rain streak information for enhancing the training.

5 Conclusion

We proposed a novel semi-supervised GAN-based deraining network that can apply both the synthetic and real-world rainy images to a uniform network using two supervised and unsupervised processes. Based on the semi-supervised rain mask learner that makes the real images contribute more rain streak information and paired discriminator, our network can clearly perform better than the recently proposed state-of-the-art method SSTL, especially on real-world images. We also contribute a new real image dataset Real200 as a byproduct, and based on Real200 we can obtain enhanced SID results on both synthetic and real images. Although enhanced results are obtained, we still cannot balance the generators G_s and G_r appropriately, since the differences of the rain streaks in synthetic and real image domains make GAN-based model difficult to converge. In future, we will also study better training architectures and skills for the semi-supervised SID, and discover more connections between the two domains.

Acknowledgments

This work is partially supported by the National Natural Science Foundation of China (61672365, 61732008, 61725203,

61622305, 61871444 and 61806035) and the Fundamental Research Funds for Central Universities of China (JZ2019-HGPA0102). Zhao Zhang is the corresponding author.

References

- [Zhu *et al.*, 2017] J. Zhu, T. Park, P. Isola, and A. A. Efros. Unpaired image-to-image translation using cycle-consistent adversarial networks. In *IEEE International Conference on Computer Vision (ICCV)*, 2017.
- [Fu *et al.*, 2017] X. Fu, J. Huang, D. Zeng, Y. Huang, X. Ding, and J. Paisley. Removing Rain from Single Images via a Deep Detail Network. In *Proceedings of the IEEE Conference on Computer Vision and Pattern Recognition (CVPR)*, Honolulu, HI, pp. 1715-1723, 2017.
- [He *et al.*, 2016] K. He, X. Zhang, S. Ren, and J. Sun. Deep Residual Learning for Image Recognition. In *Proceedings of the IEEE Conference on Computer Vision and Pattern Recognition (CVPR)*, pp.770-778, 2016.
- [Li *et al.*, 2016] Y. Li, R. T. Tan, X. Guo, J. Lu, and M. S. Brown. Rain Streak Removal Using Layer Priors. In *Proceedings of the IEEE Conference on Computer Vision and Pattern Recognition (CVPR)*, Las Vegas, NV, pp. 2736-2744, 2016.
- [Luo *et al.*, 2015] Y. Luo, Y. Xu, and H. Ji. Removing Rain from a Single Image via Discriminative Sparse Coding. In *Proceedings of the IEEE International Conference on Computer Vision (ICCV)*, Santiago, pp. 3397-3405, 2015.
- [Zhang *et al.*, 2017] H. Zhang, V. Sindagi, and V. M. Patel. Image de-raining using a conditional generative adversarial network. In *Proceedings of the IEEE Conference on Computer Vision and Pattern Recognition (CVPR)*, Honolulu, HI, pp. 247-256, 2017.
- [Zhang and Patel, 2018] H. Zhang and V. M. Patel. Density-Aware Single Image De-raining Using a Multi-stream Dense Network. In *Proceedings of the IEEE Conference on Computer Vision and Pattern Recognition (CVPR)*, Salt Lake City, UT, pp. 695-704, 2018.
- [Yang *et al.*, 2017] W. Yang, R. T. Tan, J. Feng, J. Liu, Z. Guo, and S. Yan. Deep Joint Rain Detection and Removal from a Single Image. In *Proceedings of the IEEE Conference on Computer Vision and Pattern Recognition (CVPR)*, Honolulu, HI, pp. 1685-1694, 2017.
- [Wang *et al.*, 2004] Z. Wang, A. C. Bovik, H. R. Sheikh, and E. P. Simoncelli. Image quality assessment: from error visibility to structural similarity. *IEEE Transactions on Image Processing*, vol. 13, no. 4, pp. 600-612, 2004.
- [Johnson *et al.*, 2016] J. Johnson, A. Alahi, and F. L. Perceptual losses for real-time style transfer and super-resolution. *arXiv preprint arXiv:1603.08155*, 2016.
- [Paszke *et al.*, 2017] A. Paszke, S. Gross, S. Chintala, G. Chanan, E. Yang, Z. DeVito, Z. Lin, A. Desmaison, L. Antiga, and A. Lerer. Automatic differentiation in pytorch. In *NIPS Autodiff Workshop: The Future of Gradient-based Machine Learning Software and Techniques*, 2017.
- [Kingma and Ba, 2015] D. P. Kingma and J. Ba. Adam: A method for stochastic optimization. In *Proceedings of the International Conference on Learning Representation (ICLR)*, San Diego, CA, USA, 2015.
- [Huynh-Thu and Ghanbari, 2008] Q. Huynh-Thu and M. Ghanbari. Scope of validity of PSNR in image/ video quality assessment. *Electronics Letters*, vol. 44, no. 13, pp. 800-801, 2008.
- [Wei *et al.*, 2019] Y. Wei, Z. Zhang, H. Zhang, R. Hong, and M. Wang. A Coarse-to-Fine Multi-stream Hybrid Deraining Network for Single Image Deraining. In *Proceedings of the IEEE International Conference on Data Mining(ICDM)*, 2019.
- [Wei *et al.*, 2019] W. Wei, D. Meng, Q. Zhao, Z. Xu, Y. Wu. Semi-supervised transfer learning for image rain removal. In *Proceedings of IEEE Conference on Computer Vision and Pattern Recognition (CVPR)*, pp. 3877-3886, 2019.
- [Qian *et al.*, 2018] R. Qian, R. Tan, W. Yang, J. Su, and J. Liu. Attentive generative adversarial network for raindrop removal from a single image. In *Proceedings of the IEEE Conference on Computer Vision and Pattern Recognition (CVPR)*, pp. 1-1, 2018.
- [Simonyan and Zisserman, 2015] K. Simonyan and A. Zisserman. Very deep convolutional networks for large-scale image recognition. In *Proceedings of the International Conference on Learning Representation(ICLR)*, 2015.
- [Goodfellow *et al.*, 2014] I. Goodfellow, J. Pouget-Abadie, M. Mirza, B. Xu, D. Warde-Farley, S. Ozair, A. Courville, and Y. Bengio. Generative adversarial nets. In *Advances in Neural Information Processing Systems(NeurIPS)*, pp. 2672-2680, 2014.
- [Wang *et al.*, 2019] H. Wang, M. Li, Y. Wu, Q. Zhao, and D. Meng. A Survey on Rain Removal from Video and Single Image. *arXiv preprint arXiv:1909.08326*, 2019.
- [Lee *et al.*, 2018] H. Lee, H. Tseng, J. Huang, M. Singh, and M. Yang. Diverse Image-to-Image Translation via Disentangled Representations. In *Proceedings of the European Conference on Computer Vision (ECCV)*, 2018.
- [Deng *et al.*, 2009] J. Deng, W. Dong, R. Socher, L. Li, K. Li, and F. Li. ImageNet: A Large-Scale Hierarchical Image Database. In *Proceedings of the IEEE Conference on Computer Vision and Pattern Recognition (CVPR)*, 2009.
- [Zhang and Patel, 2017] H. Zhang, V. Patel. Convolutional Sparse and Low-Rank Coding-Based Rain Streak Removal. In *Proceeding of the IEEE Winter Conference on Applications of Computer Vision (WACV)*, Santa Rosa, CA, pp. 1259-1267, 2017.
- [Gu *et al.*, 2019] Q. Gu, G. Wang, M. Chiu, Y. Tai, and C. Tang. LADN: Local Adversarial Disentangling Network for Facial Makeup and De-Makeup. In *Proceedings of the IEEE International Conference on Computer Vision (ICCV)*, 2019.